

Polymeric waveguides with embedded micro-mirrors formed by Metallic Hard Mold

Xinyuan Dou^a, Xiaolong Wang^b, Haiyu Huang^a, Xiaohui Lin^a, Duo Ding^a, David Z. Pan^a
and Ray T. Chen^{a*}

^a Department of Electrical and Computer Engineering, University of Texas at Austin, Austin, TX, 78758, USA

^b Omega Optics, Inc. Austin, TX 78759

*chen@ece.utexas.edu

Abstract: In this paper, we presented fabrication of nickel based metal mold with 45° tilted surfaces on both ends of the channel waveguide through electroplating process. To obtain a precise 45° tilted angle, a 50μm thick SU-8 layer was UV exposed under de-ionized water, with repeatable error control of 0.5°. The polymeric waveguide array with 45° micro-mirrors, which is formed by a UV imprinting method with the fabricated metallic mold, shows total insertion losses around 4dB, propagation loss around 0.18dB/cm and 75% coupling efficiency.

©2009 Optical Society of America

OCIS codes: (130.5460) Polymer waveguides; (120.4610) Optical fabrication; (220.4000) Microstructure fabrication.

References and Links

1. R. T. Chen, Lei Lin, Chulchae Choi, Y. J. Liu, B. Bihari, L. Wu, S. Tang, R. Wickman, B. Picor, M. K. Hibb-Brenner, J. Bristow, and Y. S. Liu, "Fully Embedded Board level Guided-wave Optoelectronic Interconnects," *Proc. IEEE* **88**(6), 780–793 (2000).
2. A. V. Krishnamoorthy, and D. A. B. Miller, "Scaling optoelectronic-VLSI circuits into the 21st century: A technology roadmap," *IEEE J. Sel. Top. Quantum Electron.* **2**(1), 55–76 (1996).
3. E. Mohanmed, A. Alduino, T. Thomas, H. Braunisch, D. Lu, J. Heck, A. Liu, I. Young, B. Barnett, G. Vandentop, and R. Mooney, "Optical interconnect system integration for ultra-short-reach applications," *J. Intel. Technol.* **8**(2), 115–127 (2004).
4. L. Wang, X. Wang, W. Jiang, J. Choi, H. Bi, and R. T. Chen, "45° polymer-based total internal reflection coupling mirrors for fully embedded intraboard guided wave optical interconnects," *Appl. Phys. Lett.* **87**(14), 141110 (2005).
5. X. Wang, W. Jiang, L. Wang, H. Bi, and R. T. Chen, "Fully Embedded Board-Level Optical Interconnects From Waveguide Fabrication to Device Integration," *J. Lightwave Technol.* **26**(2), 243–250 (2008).
6. M. Hikita, R. Yoshimura, M. Usui, S. Tomaru, and S. Imamura, "Polymeric optical waveguides for optical interconnections," *Thin Solid Films* **331**(1), 303–308 (1998).
7. S. H. Hwang, W.-J. Lee, J. W. Lim, K. Y. Jung, K. S. Cha, and B. S. Rho, "Chip- and board-level optical interconnections using rigid flexible optical electrical printed circuit boards," *Opt. Express* **16**(11), 8077–8083 (2008).
8. C. Choi, L. Lin, Y. Liu, J. Choi, L. Wang, D. Haas, J. Magera, and R. T. Chen, "Flexible optical waveguide film fabrications and optoelectronic devices integration for fully embedded board-level optical interconnects," *J. Lightwave Technol.* **22**(9), 2168–2176 (2004).
9. F. Wang, F. Liu, and A. Adibi, "45 Degree Polymer Micromirror Integration for Board-Level Three-Dimensional Optical Interconnects," *Opt. Express* **17**(13), 10514–10521 (2009).
10. W. J. Lee, S. H. Hwang, J. W. Lim, and B. S. Rho, "Polymeric Waveguide Film With Embedded Mirror for Multilayer Optical Circuits," *IEEE Photon. Technol. Lett.* **21**(1), 12–14 (2009).
11. J. Van Erps, N. Hendrickx, C. Debaes, P. Van Daele, and H. Thienpont, "Discrete Out-of-Plane Coupling Components for Printed Circuit Board-Level Optical Interconnections," *IEEE Photon. Technol. Lett.* **19**(21), 1753–1755 (2007).
12. N. Hendrickx, J. Ü. Van Erps, E. Bosman, C. Debaes, H. Thienpont, and P. Van Daele, "Embedded Micromirror Inserts for Optical Printed Circuit Boards," *IEEE Photon. Technol. Lett.* **20**(20), 1727–1729 (2008).

1. Introduction

In the past many years, optical interconnects were extensively investigated to provide high-density and high speed data transmission [1–10]. Traditional electrical circuits have the disadvantage of bandwidth limitations, electromagnetic interference, and skin effect [2]. Polymer based fully embedded board level optical interconnect attracts more and more

attention because of its low transmission loss, compatibility with printed circuits board (PCB) and high speed data transmission [3]. In the board level optical interconnect, 45° total internal reflection (TIR) micro-mirrors play a significant role in vertical-horizontal optical coupling [4–12]. Many techniques can be used to fabricate the 45° micro-mirrors, such as polishing and soft molding [4,5], sawing [6,7], direct cutting [8], tilted exposure [9], ultra-precision machining (UPM) method [10] and Deep Proton Writing(DPW) method [11,12]. The cutting or sawing method fabricated 45° surfaces separately, which has a disadvantage of low repeatability. In the paper of Wang *et al* [9], they also used the tilted exposure under D.I. water to fabricate the waveguide devices with 45° angle structures using the LightLink™ photopolymer. They used the air/polymer interface instead of metals as the coupling mirror, which has low coupling efficiency. UPM method used a very expensive ultra-precision machining system to form the metal hard mold, which is not suitable for every user from the cost point of view. In this letter, we presented a very economic method with combination of tilted exposure and metal electroplating process, to achieve the metallic optical waveguide hard mold and the 45° total internal reflection (TIR) micro-mirror surfaces simultaneously. Once a high quality metallic mold was successfully fabricated, it can be used in the waveguide fabrication for many times, which can reduce the cost of each device further more and also guarantee the quality of the embedded 45° Au-coated mirrors.

In the process of optical waveguide metal mold fabrication, the waveguide pre-mold(50um×50um cross section) with reverse 45° surfaces on both ends was first prepared using SU-8 (from MicroChem) through tilted exposure under D.I. water. SU-8 layer acted as a scarified layer which was removed after electroplating process. After achieving the waveguide pre-mold, metal Ni was electroplated into SU-8 defined waveguide trenches. As the electroplating process was finished, SU-8 was removed completely using remover PG (from MicroChem). In this way the metal mold with 45° surfaces on both ends was successfully fabricated. Polymeric optical waveguide array with fully embedded 45° total internal reflection (TIR) micro-mirrors was formed by UV imprinting technique using the fabricated hard mold. The metal Ni mold fabrication and polymeric waveguide imprint process is schematically shown in Fig. 1(a) and (b), respectively.

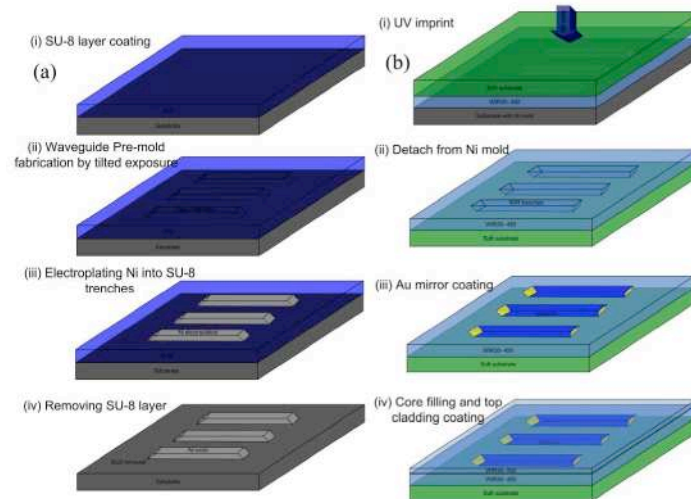


Fig. 1. Schematic view of whole process of (a) Ni mold fabrication and (b) polymeric waveguide imprint

2. Preparation of SU-8 pre-mold with 45° surfaces

In order to fabricate Ni metal mold through electroplating method, we first prepared the pre-mold for the waveguide, which defines the shape and structure of the waveguide metal mold.

A negative photoresist SU-8 2025 was used for the pre-mold, which was spin-coated with a thickness of 50 μ m. The refractive index of SU-8 is about 1.62 at 365nm. If directly exposed in air, the maximum refraction angle within SU-8 is only 34.2°. This process is simply governed by Snell's law: $n_{medium} \times \sin(\theta_i) = n_{SU-8} \times \sin(\theta_r)$, θ_i and θ_r are the incident and refractive angles in the medium and SU-8, respectively. To achieve 45° refractive angle in SU-8, deionized(D.I.) water (refractive index of 1.34 at 365nm) was selected as the input media. The tilted exposure setup is shown in Fig. 2. When the UV light (mercury lamp) is vertically shined onto the D.I. water, the tilted angle for the substrate in water is 58.7° to make 45° refraction angle within SU-8.

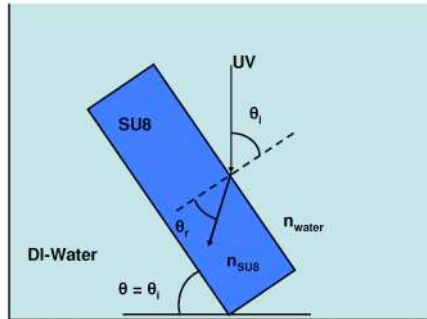


Fig. 2. Schematic view of the tilted exposure on SU-8 in DI-water (θ_i and θ_r are the incident and refractive angles, respectively.)

There are a few steps in SU-8 pre-mold preparation process, as shown in Fig. 3: (1) evaporate-coating 10nm/100nm of Ti/Au electroplating seed layer on the substrate using e-beam evaporator. (2) Spin-coating a thin layer of Omnicoat and 50 μ m thick of SU-8 2025, prebake on a hotplate at 65°C for 2-3min then ramp to 95°C, stay at 95°C for 6min, then cooling down to room temperature. Omnicoat was used in order to remove cross-linked SU-8 in remover PG completely after electroplating. (3) Using the waveguide mask(50 μ m in width, 250 μ m in period, 65mm in length) to do the vertical exposure. A UV filter was used to cut off the light below 350nm. (4) Using a small window mask, to do the 1st and 2nd tilted exposure under D.I. water. A metal stage with 58.7° angle was used to hold the sample and the photomask. These two exposures were identical except that the small window was moved from one end of the waveguide patterns to the other end. During the exposure process, the air bubbles need to be removed completely to avoid the unexpected diffractions. So index match material, such as silicone oil, was used between the photomask and the SU-8 film. After exposure, silicone oil can be easily rinsed away by DI-water. (5) Post-exposure-bake(PEB) was carried out ramping from 50°C to 95°C, staying at 95°C for 6min, then cooling down to room temperature on hotplate itself. At last the sample was developed. Before doing Ni electroplating, SU-8 residues inside the waveguide trenches were removed completely by O₂ plasma ash for a few minutes. No damage on the SU-8 pre-mold was observed after O₂ plasma ash.

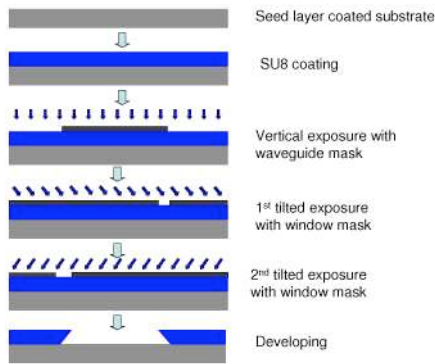


Fig. 3. Schematic process of SU-8 pre-mold with 45° surfaces fabrication

Figure 4 shows the optical pictures of SU-8 pre-mold waveguide trenches in (a) small and (b) large magnification. The black squares at the end of waveguide array are corresponding to the reverse 45° surfaces. They are shown black because the light was not reflected back into the microscope but to waveguide trench direction.

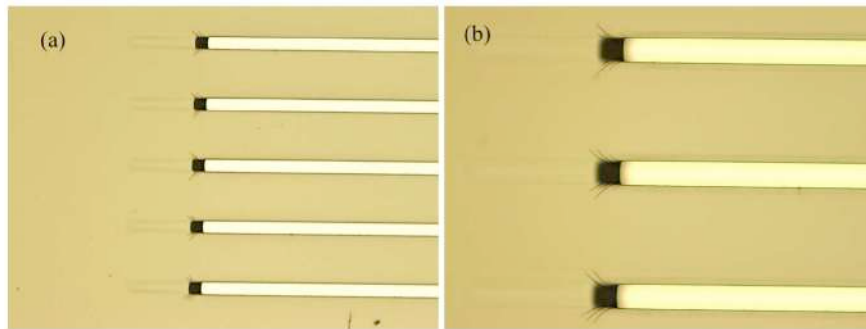


Fig. 4. Top view of SU-8 pre-mold in (a) small magnification and (b) large magnification

In order to inspect the quality of the waveguide and 45° surfaces on both ends of the waveguide trenches, the fabricated SU-8 pre-mold samples were cleaved in the perpendicular and parallel direction of the waveguide trench, respectively. The cleaved samples were sputtered with Au and viewed under Scanning Electron Microscope (SEM). Figure 5 shows the typical SEM pictures of SU-8 pre-mold. Figure 5(a) shows the cross section view in perpendicular direction of the waveguide trench. The inset of Fig. 5(a) shows a perfect vertical shape of the waveguide trench. Figure 5(b) shows the cross section view in parallel direction of the waveguide trench. The cleaving line must be exactly in the middle of the trench in order to view the 45° surfaces directly, as shown in Fig. 5(b). The 45° surfaces angle was measured (inset of Fig. 5(b)) to be 45.5°, only 1% deviating from the designed value. Based on several rounds of fabrication, this result is repeatable. It also confirms our theoretical calculation on the tilted exposure in water.

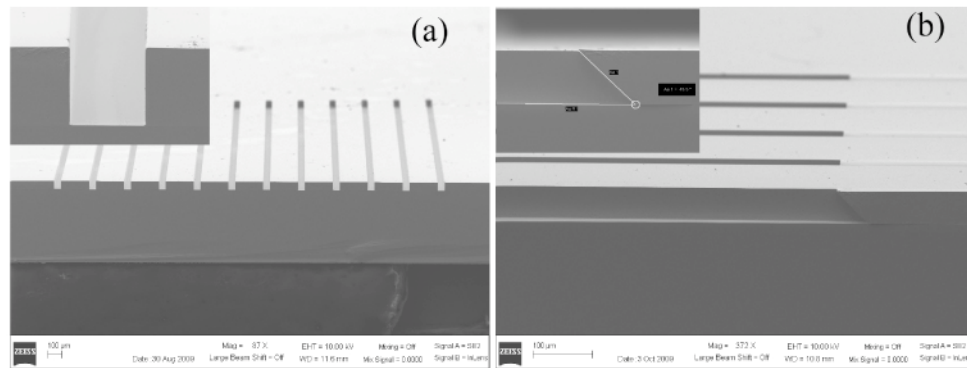


Fig. 5. SEM pictures of SU-8 pre-mold cross section with 45° surfaces at the end of the waveguide in the direction (a) perpendicular and (b) parallel to the waveguide trench.

3. Electroplating Ni metal hard mold

After successfully achieving SU-8 pre-mold with reverse 45° surfaces on both ends, metal Ni was electroplated into the waveguide trenches. The Ni electroplating kit was purchased from Caswell Inc. In order to achieve a strong adhesion between the Ni mold and the seed layer, very small plating current density (1-2mA/cm²) was first used at the start, then large current density (10mA/cm²). At the end of plating process, small current density (1-2mA/cm²) was used again to achieve a good terminating surface. Plating speed is around 120nm/min at 10mA/cm². To achieve 50um of thickness, the typical plating time is around 6-7hrs. After finishing Ni plating process, SU-8 pre-mold was removed from the substrate with Remover PG and its residues were removed by O₂ plasma.

Figure 6 shows the SEM pictures of plated waveguide metal Ni hard mold on Si substrate. Figure 6(a) gives a top view of the Ni hard mold with 12 channels. The width of the waveguide was measured to be 49.1um. To measure the actual slant angle of 45° surfaces at the mold waveguide ends, the sample was cleaved between two mold waveguide lines. Figure 6(b) gives a side view of waveguide mold. We measured actual slant angle of 45° surfaces to be 44.5° (Fig. 6(c)), which is highly consistent with SU-8 pre-mold reverse angle measurement. This result is also repeatable based on our experiment results. Figure 6(d) gives the surface profile image of the waveguide metal mold, which was scanned at the center area by Dektak 150 Surface Profiler. The heights of 12 channels are around 50um with very good uniformity. The height at the end of waveguide is a little larger than that in the middle because in the electroplating process the electric field is stronger at the end than that in the middle. More Ni ions are attracted and Ni grows faster at the ends region. This small difference was proved to have no negative effect on the devices performance.

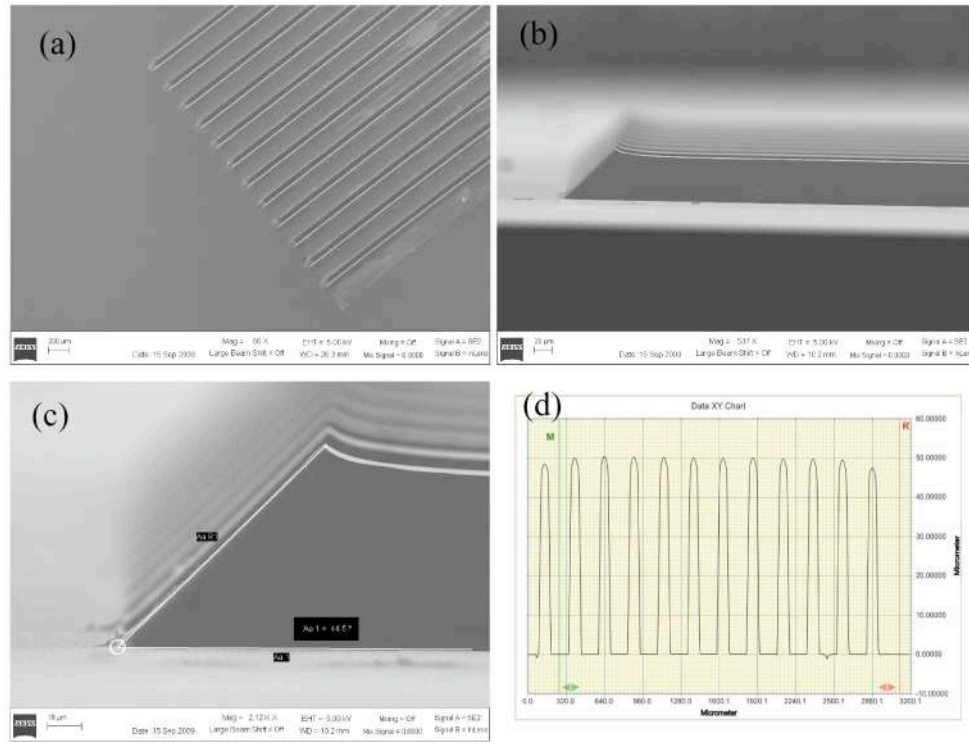


Fig. 6. (a) Top view SEM picture of the Ni hard mold with 12 channels on Si substrate. (b) Side view SEM picture of Ni hard mold on Si substrate. (c) Large magnification of the side view of 45 surfaces. The angle shown is 44.5°. (d) Surface profile image of the waveguide metal mold.

4. Polymeric waveguide device fabrication

Using the electroplated Ni waveguide hard mold, we successfully fabricated the waveguide devices by UV imprint technique. UV curable polymers are WIR30 series (from ChemOptics), WIR30-450(index at 850nm: 1.45) for the bottom cladding and top cladding, WIR30-470(index at 850nm: 1.47) for the waveguide core. TEONEX thin film (from Dupont Teijin Films Inc.) with thickness of 200um was used as the TOPAS substrate.

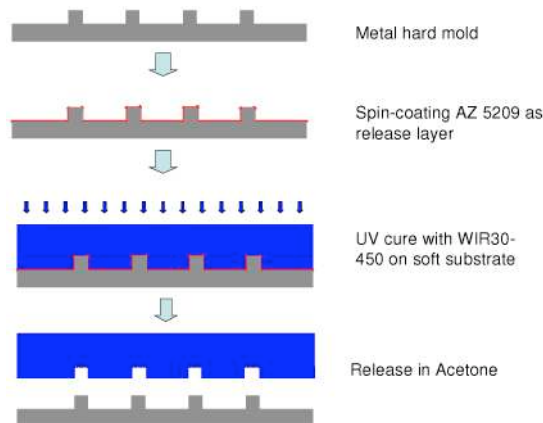


Fig. 7. Schematic of waveguide device fabrication using UV imprint technique

The process for UV imprint is shown in Fig. 7: (1) Spin-coating and bake ZAP-1020 as the adhesion promoter onto the TOPAS film substrate. (2) Spin-coating WIR30-450 for bottom cladding, UV cured in N₂. (3) Spin-coating AZ5209 on Ni hard mold as the release layer. (4) Dispense a small amount of WIR30-450 on Ni mold, and then put the film on top with pressure to remove the air bubbles. Then UV cure to make the core trenches. (5) Peel off the film substrate from Ni waveguide mold in acetone. The SEM pictures of the imprinted waveguide trenches on soft film substrate are shown in Fig. 8. (6) Evaporate-coating 200nm Au at the 45° surfaces on the waveguide trench ends. (7) Filling WIR30-470 core materials and UV cure in N₂. In filling process, excess WIR30-470 is scraped off carefully using a PDMS pad and there is no residue outside of the trenches. (8) Spin-coating WIR30-450 as top cladding, and UV cure. Hence, the polymeric waveguide with fully embedded 45° total internal reflection (TIR) micromirrors was successfully fabricated.

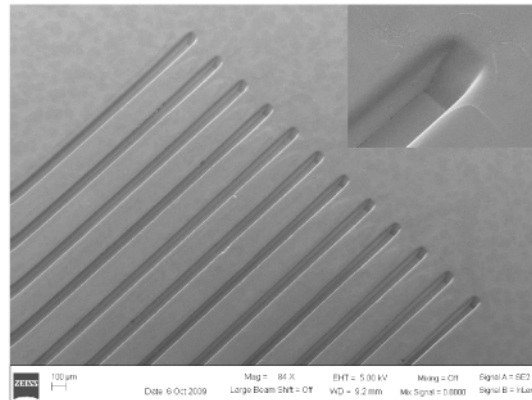


Fig. 8. SEM image of the imprinted device before core material filling (inset is in larger magnification)

5. Optical test on the device

To observe the output pattern of the imprinted waveguide, a 635nm laser source was connected to a standard 9/125um SMF with a numerical aperture of 0.12. The other end of the fiber was fixed above 45° micro-mirror region of the waveguide device. The channel length is 6.5cm. A CCD camera was connected through the microscope to export the output patterns onto the monitor. The input laser beam was shifted from 1st channel to the 12th channel in order to capture all the 12 output beam spots, which is shown in Fig. 9(a). Optical test based on the 850nm wavelength laser source was also carried out using a 850nm VCSEL diode with a 9/125um SMF pigtail, which was surface normally coupled into the waveguide through the 45° micro-mirror. The output light intensity was measured by an 850nm photodetector which was fixed just above the output end of the waveguide array. We measured the total insertion loss of each individual waveguide, calculated by the ratio of the total output power of each waveguide and the total input power of VCSEL diode at the SMF output end. The total insertion loss is around 4dB, with a deviation of 3dB for all channels. The loss difference between the channels was estimated to be due to some random factors in the imprint process. The propagation loss of each channel was measured by conventional cutting back method. First the waveguide was cleaved to be 4.0cm long. After polishing the output surface the output power for each channel was measured. Then the waveguide was cleaved again to be 2.0cm long, polishing and measurement were carried out again. By comparing with the two groups of measurement results, we can calculate the propagation loss for each channel. The results are shown in Fig. 9c. Most channels have a propagation loss from 0.1 to 0.25dB/cm. The average value is 0.18dB/cm. Assuming the input and output micro-mirrors have the same coupling efficiency, the coupling losses are calculated to be between 1.3dB and 3.0dB (Fig. 9d), which means the 45° TIR micro mirrors have a coupling efficiency of 75%. Comparing

with some reported values [4,5,11,12], further optimization of mold and device fabrication is need to achieve higher coupling efficiency.

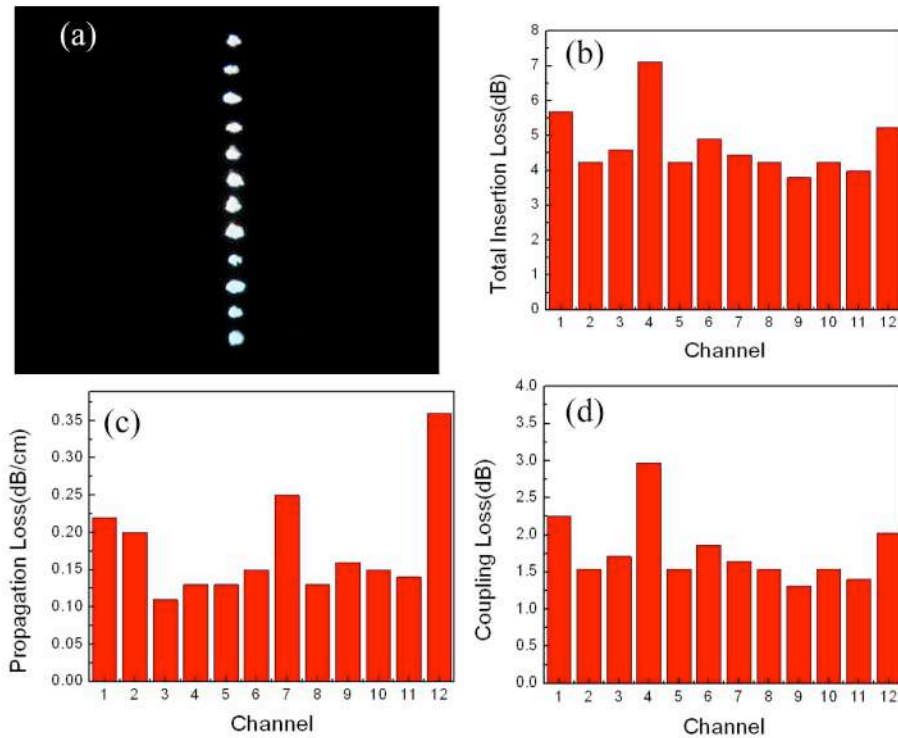


Fig. 9. (a) Output image from screen (b) total insertion loss (c) measured propagation loss and (d) calculated coupling loss for 45° TIR micro-mirrors.

6. Conclusion

In summary, we have successfully fabricated SU-8 pre-mold for waveguide array with reversed 45° surfaces on both ends by tilted exposure under D.I. water. Waveguide metal mold with 45° surfaces was achieved by electroplating Ni into the SU-8 pre-mold trenches. SU-8 layer was removed after electroplating process. The actual slant angle of the mold 45° surfaces is 44.5°. After obtaining the metal hard mold, polymeric waveguide device based on WIR30 series of UV curable photopolymers was obtained by a UV imprint technique. The total insertion loss at 850nm of an individual polymeric waveguide was around 4dB and the average propagation loss is around 0.18dB/cm. The embedded 45° micro-mirrors have a coupling efficiency of 75%.

Acknowledgements

This work is supported by the National Science Foundation. The fabrication and characterization facilities at UT MRC are supported through NNIN program.